

Original Article

Efficacy and prognosis of multimodal angiography-interventions for chronic pulmonary artery stenosis and pulmonary hypertension

Zhongyuan Zhang¹, Xian Zhang², Feng Duan², Zhijun Song², Shan Ma²

¹*Interventional Therapy Center, Zhangye Second People's Hospital, No. 93, Xihuan Road, Ganzhou District, Zhangye 734000, Gansu, China;* ²*Department of Interventional Medicine, Zhangye Second People's Hospital, No. 93, Xihuan Road, Ganzhou District, Zhangye 734000, Gansu, China*

Received August 14, 2025; Accepted November 25, 2025; Epub December 15, 2025; Published December 30, 2025

Abstract: Objective: To explore the effects of multimodal endoluminal interventional technology combined therapy on clinical efficacy, pulmonary vascular resistance (PVR), pulmonary microvessel density (MVD), and long-term prognosis in patients with chronic pulmonary artery stenotic pulmonary hypertension (CPAS-PH). Methods: This retrospective analysis included 117 CPAS-PH patients (January 2019 - December 2022) who received the combined therapy. They were divided into a control group (n=50) and an observation group (n=67). Baseline data, preoperative and 6-month postoperative PVR, MVD, left ventricular ejection fraction (LVEF), left ventricular end-diastolic diameter (LVEDD), 6-minute walking distance (6MWD), N-terminal pro-B-type natriuretic peptide (NT-proBNP), and complications were collected. Kaplan-Meier method was used to analyze 2-year survival, Cox regression to identify independent prognostic factors and nomogram and ROC curve to verify diagnostic efficacy. Results: The observation group had a lower 6-month postoperative PVR, LVEDD, NT-proBNP, adverse reaction rate, and 2-year mortality (all $P<0.001$), but higher MVD, LVEF, 6MWD, and follow-up duration (all $P<0.001$) than the control group. Multivariate Cox analysis showed $PVR \geq 5.305$ WU ($HR=4.324$, 95% CI: 1.666-11.221, $P=0.003$), $LVEDD \geq 56.95$ mm ($HR=3.632$, 95% CI: 1.110-11.887, $P=0.033$) were prognostic factors. Having $MVD \geq 14.5$ ($HR=0.279$, 95% CI: 0.113-0.685, $P=0.005$) and $LVEF \geq 39.34\%$ ($HR=0.093$, 95% CI: 0.024-0.354, $P=0.001$) were protective factors. The nomogram and ROC curve confirmed good diagnostic efficacy. Conclusion: Multimodal endoluminal interventional combined therapy effectively reduces PVR, promotes pulmonary microvascular remodeling, and improves cardiac function and exercise tolerance, with favorable long-term prognosis. Postoperative 6-month PVR, MVD, LVEF, and LVEDD are important evaluation indicators.

Keywords: Chronic pulmonary artery stenosis pulmonary hypertension, multimodal vascular endoluminal imaging, interventional procedures, pulmonary vascular resistance, pulmonary micro-vessel density, prognostic analysis

Introduction

Chronic pulmonary artery stenosis (CPAS) refers to the loss of pulmonary artery lumen area caused by various factors, with common causes including endovascular obstruction, extravascular compression, and vascular wall inflammatory hyperplasia [1]. Without intervention, this condition can lead to the development of chronic pulmonary artery stenotic pulmonary hypertension (CPAS-PH) [2]. Among clinical treatments for CPAS-PH, traditional pharmacotherapy, while capable of dilating pulmonary vessels and improving cardiac function, is often

ineffective in patients with moderate-to-severe pulmonary stenosis, rendering it difficult to effectively reduce pulmonary vascular resistance (PVR) and prevent disease progression [3]. Interventional procedures, such as percutaneous pulmonary arterioplasty (PPA), are currently important approaches for CPAS treatment. While this intervention can significantly improve symptoms, exercise capacity, and hemodynamic status in patients affected by CPAS-PH, it is associated with a high postoperative restenosis rate, and long-term prognosis remains unsatisfactory [4, 5]. Thus, the search for more effective therapeutic strategies for

Multimodal angiography -for chronic PH

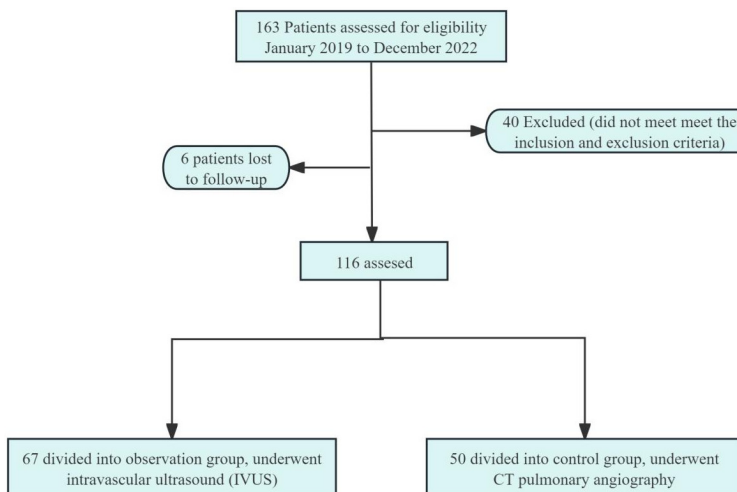


Figure 1. Flow chart illustrating patient selection.

CPAS-PH--ones that can significantly reduce PVR, promote pulmonary microvascular remodeling, and improve patient prognosis--has become the focus of current research on this condition.

Vascular interventional therapy relies on imaging assessment. Traditional imaging techniques such as digital subtraction angiography (DSA), CT angiography (CTA), and magnetic resonance angiography (MRA) can accurately visualize vascular anatomy. However, they have notable limitations in real-time intraoperative dynamic assessment and post-interventional efficacy monitoring, and these are shortcomings that fail to meet the requirements for precise treatment [6]. With the advancement of imaging technology in recent years, multimodal vascular intraluminal imaging has developed rapidly. It integrates optical coherence tomography (OCT), intravascular ultrasound (IVUS), and their dual-modality system (IVUS-OCT). While acquiring accurate vascular structural information on patients, it significantly improves the capacity to comprehensively evaluate patients' lesions [7]. Several studies have demonstrated that the use of advanced imaging technologies (e.g., intravascular ultrasound) to guide cardiovascular interventional procedures of varying severity and types supports the formulation of individualized treatment regimens and enhances the precision and safety of therapy [8, 9]. However, their role in the therapeutic efficacy for patients with CPAS-PH, as well as their effect on reducing PVR and promoting pul-

monary microvascular remodeling in these patients, has not been systematically evaluated in depth.

Therefore, we undertook a retrospective study on CPAS-PH patients treated in Zhangye Second People's Hospital. It deeply integrates multimodal intravascular imaging technology with endoluminal interventional therapy, uses the complementary advantages of multimodal imaging to achieve accurate lesion assessment and real-time therapeutic guidance, focuses on PVR and MVD indicators, and systematically

analyzes the combined regulatory effects of multimodal integrated therapy on these two measurements. In addition, it identifies independent factors affecting long-term prognosis through survival analysis and model construction, verifies their diagnostic efficacy, attempts to establish a prognosis evaluation tool based on objective indicators, and thereby provides a quantitative basis for accurate clinical prognosis assessment.

Materials and methods

Patient selection

A total of 163 patients diagnosed with CPAS complicated with PH in Zhangye Second People's Hospital from January 2019 to December 2022 were retrospectively selected. Among them, 40 patients who did not meet the inclusion and exclusion criteria were excluded, and another 6 patients lost to follow-up were also excluded. Finally, a total of 117 patients were assessed for the study (Figure 1). They were divided into an observation group (n=67) and a control group (n=50) according to different treatment methods. Inclusion criteria: (1) definite diagnosis of CPAS confirmed by CTA; (2) conformity to the diagnostic criteria for pulmonary hypertension [10]; (3) suitable for multimodal endoluminal intervention by imaging assessment; (4) aged 18-80 years; (5) conformity to the diagnostic criteria for pulmonary hypertension. Exclusion criteria: (1) Combination of severe congenital heart disease, car-

diomyopathy, valvular disease and other serious cardiac diseases; (2) combination of malignant tumors, severe hepatic and renal insufficiency, and coagulation dysfunction, etc.; (3) acute myocardial infarction, stroke, or pulmonary embolism in the last 3 months; (4) allergy to the devices or drugs used in the interventional therapy; (5) presence of psychiatric disease or cognitive dysfunction. This study was approved by the Ethics Committee of Zhangye Second People's Hospital. As a retrospective study, it was approved by the Ethics Committee to waive the requirement for obtaining informed consent from the subjects.

Surgical methods

Preoperatively, all patients underwent right heart catheterization to measure hemodynamic parameters such as pulmonary artery pressure, PVR, and cardiac output. Additionally, they received contrast-enhanced chest computed tomography (CT) and pulmonary angiography to identify the location, severity, and extent of pulmonary artery stenosis, as well as the condition of the pulmonary microvascular bed.

After all patients underwent balloon dilatation angioplasty, the observation group underwent intravascular ultrasound (IVUS) examination. Heparin Sodium injection was administered in advance to prevent thrombosis. Imaging was performed using the Boston Scientific iLab Polaris System and Opticross coronary IVUS probe. The Trace Assist software built into the ultrasound machine was used for qualitative and quantitative analysis of image information.

The control group underwent CT pulmonary angiography, which was performed using a Siemens Definition As 128-slice spiral CT scanner.

All patients were followed up for 24 months postoperatively. The follow-up methods included outpatient visits, telephone follow-ups, and inpatient reexaminations.

Outcome measures

Main outcome measures: (1) PVR of patients in both groups were measured using a Philips

IE33 ultrasound system and collected before surgery and at 6 months after surgery. (2) MVD data from patients were collected before surgery and at 6 months after surgery. The data were acquired by performing immunohistochemical staining on lung tissue specimens obtained from lung biopsy, followed by observation under a microscope.

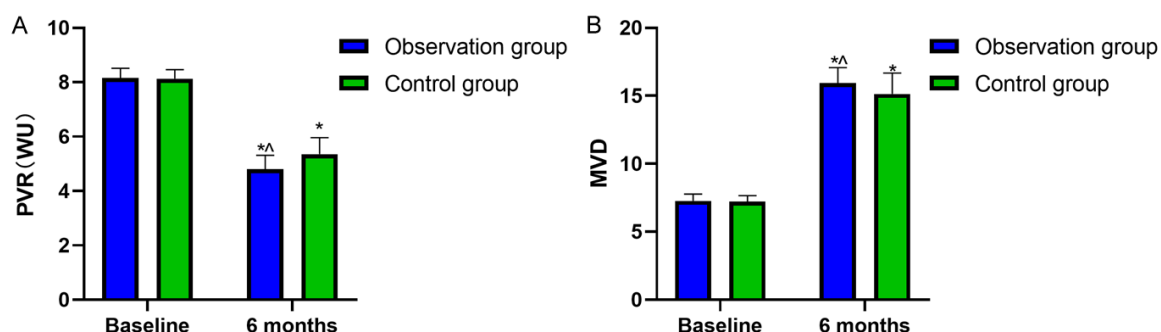
Secondary outcome measures: (1) Cardiac function indicators, including Left Ventricular Ejection Fraction (LVEF) and Left Ventricular End-Diastolic Diameter (LVEDD) were collected before surgery and at 6 months after surgery. (2) Serum N-Terminal Pro-B-Type Natriuretic Peptide (NT-proBNP) levels of patients in both groups were collected before surgery and at 6 months after surgery. (3) 6-Minute Walk Distance (6MWD) were collected before surgery and at 6 months after surgery. (4) During the postoperative follow-up period, the occurrence of complications in both groups was recorded, including pulmonary artery perforation, pulmonary artery dissection, reperfusion pulmonary edema, and arrhythmia. Additionally, the occurrence of death events and the time of death in both groups during the postoperative follow-up were collected.

Statistical analysis

Statistical analyses were conducted using SPSS 26.0 software. Continuous data were expressed as mean \pm standard deviation ($x \pm sd$). Repeated-measures analysis of variance was used to compare the data within the same group at different time points, while independent-samples t-test was applied for comparisons between groups. Categorical data were presented as rates (%), and their comparisons were performed using the chi-square (χ^2) test. New York Heart Association Stage was performed using the Mann-Whitney U test. Kaplan-Meier method was employed for survival analysis, and the Log-rank test was used to compare the survival rates between the two patient groups. Cox proportional hazards regression model was adopted to identify the influencing factors for 2-year prognostic survival in patients. Furthermore, a nomogram model was constructed and a receiver operating characteristic (ROC) curve was generated to validate its diagnostic efficacy. $P < 0.05$ was considered a significant difference.

Table 1. Comparison of general data of the two groups of patients

	Observation group (n=67)	Control group (n=50)	t/Z/χ ²	P
Age	63.31±5.73	63.3±4.95	0.010	0.992
Gender			0.206	0.650
Male	35 (52.24)	24 (48.00)		
Female	32 (47.76)	26 (52.00)		
BMI (kg/m ²)	22.68±2.45	22.69±2.19	0.023	0.982
T2DM			0.179	0.672
Yes	17 (25.37)	11 (22.00)		
No	50 (74.63)	39 (78.00)		
Hypertension			0.152	0.697
Yes	9 (13.43)	8 (16.00)		
No	58 (86.57)	42 (84.00)		
Smoking			0.033	0.855
Yes	6 (8.96)	4 (8.00)		
No	61 (91.06)	46 (92.00)		
NYHA Stage			-0.390	0.696
I	1 (1.49)	3 (6.00)		
II	20 (29.85)	10 (20.00)		
III	38 (56.71)	36 (72.00)		
IV	8 (11.94)	1 (2.00)		

**Figure 2.** PVR and MVD of 2 groups; (A) PVR of 2 groups; (B) MVD of 2 groups. Note: *, ^ mean compared to baseline, and Control group P<0.05. PVR: Pulmonary Vascular Resistance; MVD: Microvessel Density.

Results

Comparison of the general information

As shown in **Table 1**, there were no significant differences between the two groups in general information (all P>0.05).

Comparison of PVR and pulmonary MVD before and after surgery

As shown in **Figure 2**, PVR and MVD did not differ significantly between the two groups preoperatively (both P>0.05). 6 months after surgery, the PVR showed a significant downward trend and the MVD showed a significant upward trend

(all P<0.001) compared to the baseline data. Notably, the observation group had a significantly lower PVR and higher MVD than the control group, 6 months after surgery (both P<0.001).

Comparison of cardiac function indexes before and after surgery

As shown in **Figure 3**, there were no significant differences in the aforementioned indicators between the two groups before surgery (all P>0.05). At 6 months postoperatively, LVEF (**Figure 3A**) and 6MWD (**Figure 3C**) exhibited a significant increase in both groups compared to their preoperative levels, whereas LVEDD

Multimodal angiography -for chronic PH

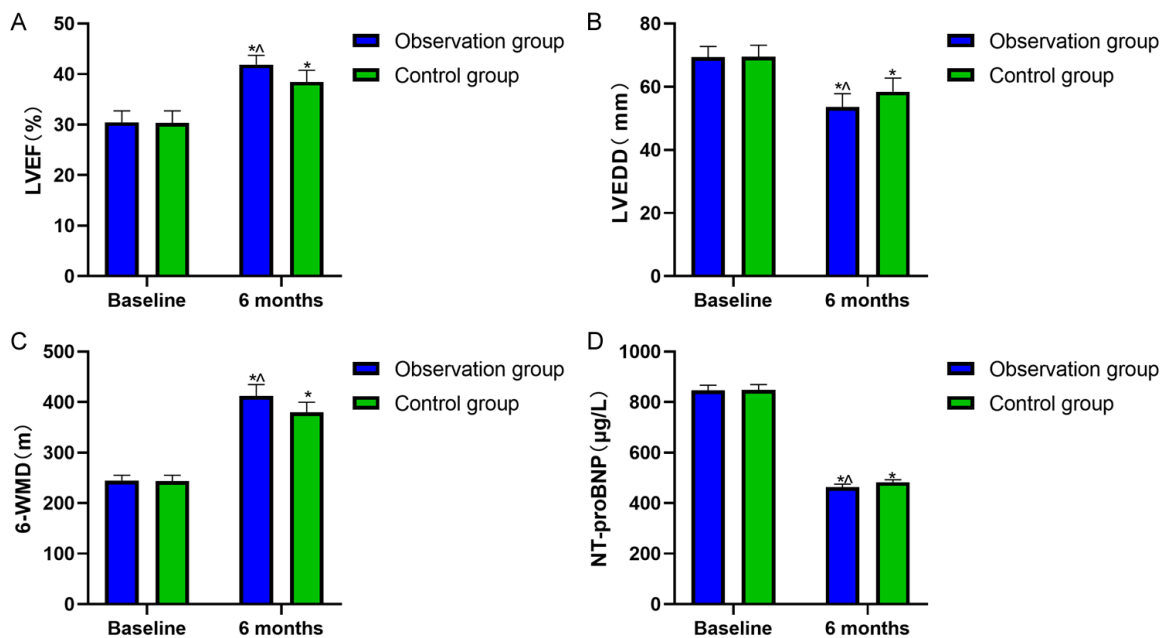


Figure 3. Cardiac function indicators of 2 groups: (A) LVEF of 2 groups; (B) LVEDD of 2 groups; (C) 6MWD of 2 groups; (D) NT-proBNP of 2 groups. Note: *, ^ mean compared to baseline, and Control group $P<0.05$. LVEF: Left Ventricular Ejection Fraction; LVEDD: Left Ventricular End-Diastolic Diameter; NT-proBNP: N-Terminal Pro-B-Type Natriuretic Peptid; 6MWD: 6-Minute Walk Distance.

Table 2. Comparison of the occurrence of complications between the two groups

	n	Pulmonary artery perforation	Pulmonary artery entrapment	Reperfusion pulmonary edema	Arrhythmias	Incidence of complications
Observation group	67	0 (0.00)	0 (0.00)	5 (7.46)	3 (4.48)	8 (11.94)
Control group	50	8 (16.00)	6 (12.00)	3 (6.00)	3 (6.00)	20 (40.00)
χ^2						12.384
P						<0.001

Table 3. Survival and follow-up time at 2 years in both groups

	Observation group (n=67)	Control group (n=50)	t/ χ^2	P
Survival at 2 years			10.840	<0.001
Survival	58 (86.57)	30 (60.00)		
Death	9 (13.43)	20 (40.00)		
Duration of follow-up (months)	21.40 \pm 2.83	18.54 \pm 4.74	4.378	<0.001

(Figure 3B) and NT-proBNP (Figure 3D) demonstrated a significant decrease (all $P<0.001$). Notably, LVEF, 6MWD and MVD in the observation group were significantly higher than those in the control group (all $P<0.001$).

Comparison of adverse reactions

As shown in Table 2, during the follow-up period, the incidence of adverse reactions in the observation group was 11.94% (8/67), which

was significantly lower than that of the control group 40% (20/50) ($P<0.001$).

2-year survival and follow-up outcomes

As shown in Table 3, all 117 CPAS-PH patients completed follow-up. The observation group had a significantly higher 2-year survival rate and longer median follow-up time than the control group (both $P<0.001$). Kaplan-Meier curve analysis (Figure 4) revealed that the observa-

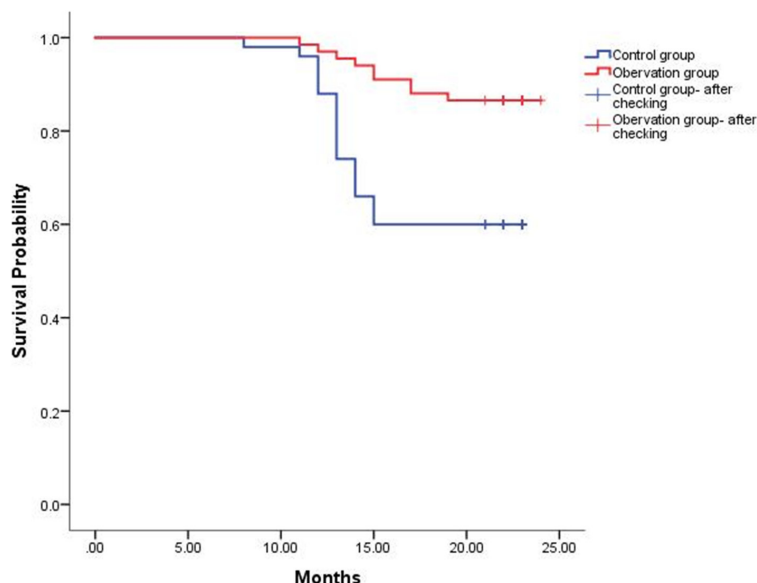


Figure 4. Kaplan-Meier curves for 2-year survival in both groups of patients.

Table 4. One-way analysis of variance of factors affecting patients' 2-year prognosis

	Survival Group (n=29)	Death Group (n=88)	$\chi^2/Z/t$	P
Age	63.21±5.31	63.34±5.44	0.112	0.911
Gender			0.071	0.789
Male	14 (48.28)	45 (51.14)		
Female	15 (51.72)	43 (48.86)		
BMI (kg/m ²)	22.73±2.32	22.67±2.35	0.120	0.935
T2DM			0.001	0.976
Yes	7 (24.14)	21 (23.86)		
No	22 (75.86)	67 (76.14)		
Hypertension			0.017	0.897
Yes	4 (13.79)	13 (14.77)		
No	25 (86.21)	75 (85.23)		
Smoking			0.159	0.890
Yes	3 (11.54)	7 (7.95)		
No	26 (88.46)	81 (92.05)		
NYHA Stage			-0.092	0.926
I	1 (3.45)	3 (3.41)		
II	7 (24.14)	23 (26.14)		
III	19 (65.52)	55 (62.50)		
IV	2 (6.90)	7 (7.95)		
PVR (WU)	5.61±0.54	4.84±0.52	6.851	<0.001
MVD	14.17±1.20	16.07±1.08	7.991	<0.001
LVEF (%)	37.64±2.35	41.35±2.03	8.203	<0.001
LVEDD (mm)	60.38±4.01	54.16±4.06	7.176	<0.001
6MWD (m)	393.34±26.41	400.38±26.37	1.246	0.215
NT-proBNP (µg/L)	474.68±13.67	471.35±14.38	1.094	0.276

tion group had a significantly longer median overall survival (log Rank $\chi^2=11.929$, $P<0.001$).

Univariate analysis of factors affecting 2-year prognosis

Among the 117 patients, 88 survivors at 2 years were assigned to the survival group, and 29 non-survivors to the death group. As shown in **Table 4**, age, gender, BMI, diabetes mellitus history, hypertension history, smoking history, and New York Heart Association classification were not significantly associated with 2-year prognosis (all $P>0.05$). In contrast, PVR, MVD, LVEF, and LVEDD were identified as potential factors influencing 2-year prognosis (all $P<0.001$).

Multifactorial Cox regression analysis of factors affecting patients' 2-year prognosis

The values assigned to each risk factor were shown presented in **Table 5**. Multivariate Cox survival analysis (**Table 6**) demonstrated that $PVR \geq 5.305$ WU ($HR=4.324$, 95% CI: 1.666-11.221, $P=0.003$) and $LVEDD \geq 56.95$ mm ($HR=3.632$, 95% CI: 1.110-11.887, $P=0.033$) were the prognostic factors affecting patients' 2-year survival, and $MVD \geq 14.5$ ($HR=0.279$, 95% CI: 0.113-0.685, $P=0.005$) and $LVEF \geq 39.34\%$ ($HR=0.093$, 95% CI: 0.024-0.354, $P=0.001$) were identified as independent protective factors for 2-year survival.

Development and validation of a prognostic nomogram

Based on the Cox regression results, four independent risk factors (PVR, MVD, LVEF,

Table 5. Risk factors and assignments

risk factors	assignment
PVR	0: <5.305 WU
	1: ≥ 5.305 WU
MVD	0: <14.5
	1: ≥ 14.5
LVEF	0: <39.34%
	1: $\geq 39.34\%$
LVEDD	0: <56.95 mm
	1: ≥ 56.95 mm

LVEDD) were used to construct a nomogram (**Figure 5A**). Among these factors, LVEF had the largest score range and the most significant contribution to risk prediction, indicating a strong correlation with prognosis. PVR, MVD, and LVEDD also showed meaningful correlations with prognostic risk. Validation of the nomogram revealed an AUC of 0.961 (95% CI: 0.926-0.997) (**Figure 5B**), and the calibration curve was close to 1 (**Figure 5C**).

ROC curve analysis of individual prognostic factors

To further validate the reliability of key indicators improved by multimodal endoluminal interventional therapy as prognostic assessment tools, this study employed ROC curve analysis to evaluate the diagnostic efficacy of 6-month postoperative PVR, MVD, LVEF, and LVEDD for the 2-year prognosis of patients with CPAS-PH. As shown in **Table 7** and **Figure 6**, all four factors exhibited significant diagnostic value: 6-month postoperative PVR (AUC=0.845, **Figure 6A**), MVD (AUC=0.877, **Figure 6B**), LVEF (AUC=0.893, **Figure 6C**), and LVEDD (AUC=0.879, **Figure 6D**).

To compare further the diagnostic efficacy among these indicators, the Delong test was used to analyze differences in AUCs (**Table 7**). Pairwise comparisons showed no statistically significant differences in AUC between any two indicators: PVR vs. MVD ($Z=0.423$, $P=0.672$), PVR vs. LVEF ($Z=0.891$, $P=0.373$), PVR vs. LVEDD ($Z=0.586$, $P=0.558$), MVD vs. LVEF ($Z=0.457$, $P=0.648$), MVD vs. LVEDD ($Z=0.062$, $P=0.951$), and LVEF vs. LVEDD ($Z=0.401$, $P=0.688$). These results indicate that while LVEF had the highest AUC, all four indicators are equally reliable for assessing 2-year prognosis in CPAS-PH patients.

Discussion

CPAS-PH is characterized by progressive pulmonary vascular stenosis, loss of pulmonary artery lumen area, and elevated pulmonary artery pressure [11, 12]. However, traditional techniques such as CTA, while capable of clearly visualizing vascular anatomy, lack the capability for real-time dynamic assessment and post-interventional efficacy monitoring, which in turn leads to significant variability in patients' therapeutic outcomes and prognosis [13]. In this study, the application of multimodal endoluminal imaging-assisted interventional therapy improved patients' 2-year survival rate and effectively controlled the occurrence of complications. In the following sections, by focusing on core indicators such as PVR and MVD, we will analyze the mechanisms through which this imaging assessment protocol enhanced the efficacy and prognosis of CPAS-PH.

Elevated PVR is one of the core pathologic features in patients with pulmonary artery stenosis. It is caused by changes such as endothelial dysfunction, pulmonary arteriolar spasm, and smooth muscle cell proliferation induced by pulmonary artery stenosis, which in turn leads to the development of pulmonary hypertension and right ventricular dysfunction, and even death in severe cases [14]. This study found that elevated PVR levels result in poor 2-year prognostic survival in patients with CPAS-PH, and multimodal intravascular imaging technology (IVUS) combined with interventional surgery could more effectively reduce vascular resistance and improve hemodynamics in patients. Two main factors contributed to this observation: (1) percutaneous transluminal pulmonary angioplasty (PTBA) can eliminate etiological factors of pulmonary artery stenosis (e.g., thrombi) within the pulmonary artery, reduce endothelial dysfunction and pulmonary arteriolar spasm caused by vascular stenosis, thereby improving patients' hemodynamics and effectively alleviating resistance [15]; (2) pulmonary angiography can only display two-dimensional luminal contours of blood vessels, and when assessing the degree of stenosis, it mostly uses adjacent "apparently normal" blood vessels as a reference, which often fails to accurately reflect the actual degree of vascular stenosis - this easily prevents PTBA from achieving optimal therapeutic effects [16, 17].

Multimodal angiography -for chronic PH

Table 6. Cox regression analysis of risk factors related to CPAS-PH

	β	StdError	Wald x^2	P	HR	95% CI
PVR \geq 5.305 WU	1.464	0.487	9.056	0.003	4.324	1.666-11.221
MVD \geq 14.5	-1.277	0.459	7.757	0.005	0.279	0.113-0.685
LVEF \geq 39.34%	-2.378	0.684	12.091	0.001	0.093	0.024-0.354
LVEDD \geq 56.95 mm	1.290	0.605	4.546	0.033	3.632	1.110-11.887

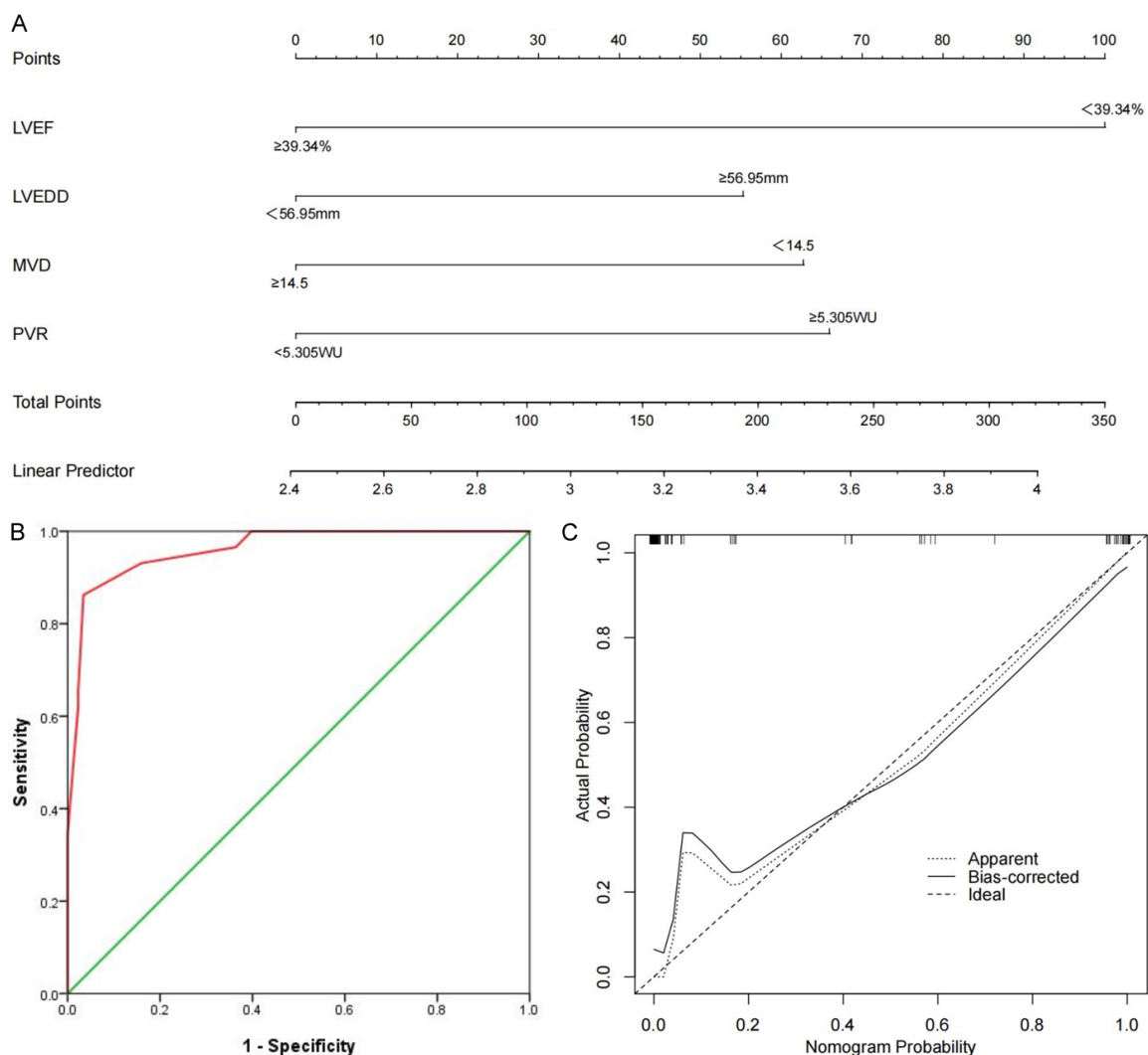


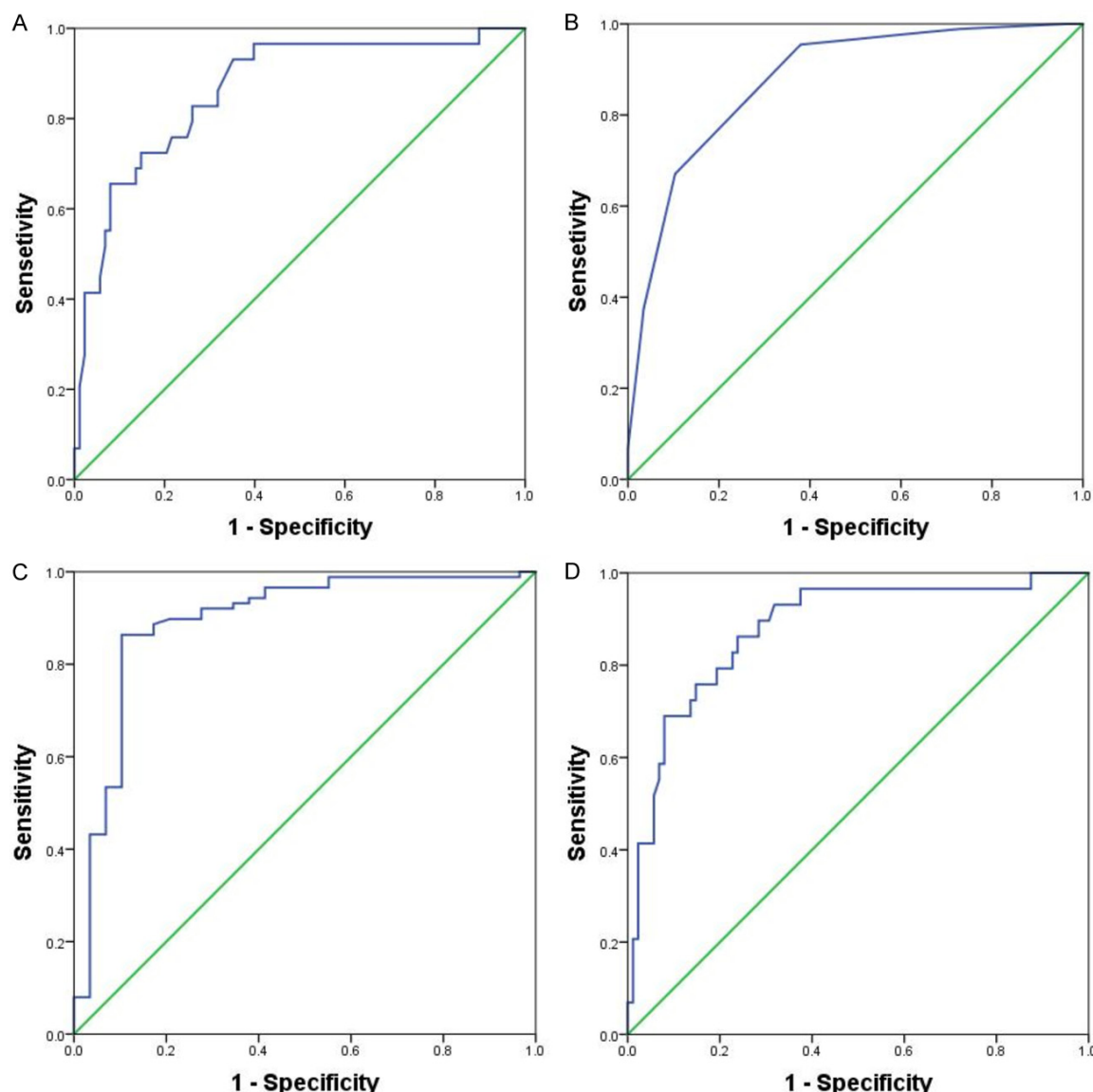
Figure 5. Nomogram model construction and diagnostic efficacy assessment: (A) Nomogram model of independent risk factors and protective factors for predicting patients' survival within 2 years; (B) ROC curves for validating Nomogram model; (C) Calibration curves for validating Nomogram model. Note: LVEF: Left Ventricular Ejection Fraction; LVEDD: Left Ventricular End-Diastolic Diameter; PVR: Pulmonary Vascular Resistance; MVD: Microvessel Density.

In contrast, IVUS can more precisely visualize pathological characteristics of the vascular wall (e.g., identifying obvious vascular stenosis), enabling PTBA to more effectively eliminate stenotic lesions and achieve more thorough therapeutic effects [18].

Elevated PVR caused by CPAS-PH tends to redirect blood flow in patients to non-stenotic or non-obstructed vascular segments, leading to a decrease in MVD and further exacerbation of the patient's condition [19]. Results of Cox analysis in this study revealed that a high MVD

Table 7. Results of ROC curves for 2-year prognosis of patients assessed by each risk and protective factor

Factor	AUC	Sensitivity	Specificity	P	95% CI	Cut-off	Youden's Index
PVR	0.864	0.759	0.852	<0.001	0.785-0.942	5.305 WU	0.611
MVD	0.877	0.955	0.621	<0.001	0.802-0.952	14.5	0.576
LVEF	0.893	0.864	0.897	<0.001	0.814-0.972	39.34%	0.761
LVEDD	0.879	0.862	0.761	<0.001	0.805-0.953	56.95 mm	0.623

**Figure 6.** ROC curves: (A) ROC curves of 2-year prognosis of patients assessed by PVR; (B) ROC curves of 2-year prognosis of patients assessed by MVD; (C) ROC curves of 2-year prognosis of patients assessed by LVEF; (D) ROC curves of 2-year prognosis of patients assessed by LVEDD. Note: PVR: Pulmonary Vascular Resistance; MVD: Microvessel Density; LVEF: Left Ventricular Ejection Fraction; LVEDD: Left Ventricular End-Diastolic Diameter.

level was a protective factor for the 2-year prognosis of CPAS-PH patients, and the combination of multimodal imaging technology and

interventional surgery can promote microvascular regeneration. The possible mechanism underlying this phenomenon is as follows: IVUS

in combination with interventional surgery can precisely ameliorate pulmonary artery stenosis in patients, thereby reducing PVR levels. This improvement in turn corrects abnormal hemodynamic circulation and pulmonary blood perfusion, further promoting the repair of microcirculation and an increase in MVD [20, 21]. This study also found that IVUS-assisted interventional surgery could improve patients' cardiac function and overall circulatory efficiency by reducing PVR and increasing MVD, which may be closely related to the cardiac compensatory mechanism. Specifically, after the reduction of pulmonary vascular resistance, right ventricular afterload is decreased, ventricular septal deviation is reduced, and left ventricular diastolic space is restored. These changes collectively lead to an increase in LVEF [22, 23]. Following the recovery of cardiac function, the increased cardiac output improves systemic oxygen supply, which in turn enhances the patient's exercise tolerance [24]. Additionally, NT-proBNP, as a ventricular wall stress-sensitive indicator, shows a decrease in its level, which further confirms the overall improvement of cardiac function [25, 26]. Cox analysis also showed that among the independent prognostic factors (LVEF and LVEDD), LVEF exerts the most significant protective effect, suggesting that cardiac reserve function is crucial for long-term survival.

In this study, the observation group had a lower postoperative complication rate, which is consistent with the findings of Kimura et al. [27] regarding IVUS-guided percutaneous coronary intervention, confirming that IVUS-assisted interventional surgery can reduce the incidence of complications in patients. Meanwhile, in terms of long-term prognosis, the observation group exhibited a higher 2-year cumulative survival rate, which is in line with the research by Gao et al. [28], demonstrating that IVUS-assisted interventional surgery could improve the long-term clinical outcome of patients with CPAS-PH. The underlying mechanism is that IVUS can improve patients' cardiac function indicators by optimizing PVR and MVD, thereby reducing the adverse effects of these indicators on patient prognosis [29]. In addition, the high-resolution imaging of IVUS enables more accurate assessment of lesions and guidance for surgery, which enhances surgical safety, effectively prevents the occurrence of periop-

erative complications such as pulmonary artery perforation, pulmonary artery dissection, and reperfusion pulmonary edema, and thus exerts a favorable effect on improving patients' long-term prognosis [30].

The limitations of this study are as follows. First, this study is a single-center retrospective study, which may have significant limitations in sample selection. Second, due to the small sample size, comparisons between different imaging modalities in multimodal technology (such as OCT and IVUS) were not conducted. Additionally, the follow-up duration of this study was only 2 years, and no research on longer-term prognostic data was performed. It is expected that in future studies, the sample size will be expanded and multicenter data will be included; meanwhile, treatment regimens will be further optimized (e.g., combining multimodal technology with targeted drugs) and the effects of different imaging modalities on patients will be compared.

In conclusion, multimodal endoluminal interventional technology combined with interventional surgery can significantly improve PVR, MVD, and cardiac function in patients with CPAS-PH, while effectively reducing the risk of complications and prolonging their survival time. Meanwhile, PVR, MVD, LVEF, and LVEDD at 6 months postoperatively can serve as reliable prognostic evaluation indicators, providing important references for clinical decision-making.

Acknowledgements

This study was supported by Gansu Province Science and Technology Plan Project (25JRRG025).

Disclosure of conflict of interest

None.

Address correspondence to: Shan Ma, Department of Interventional Medicine, Zhangye Second People's Hospital, No. 93, Xihuan Road, Ganzhou District, Zhangye 734000, Gansu, China. E-mail: mashanz@163.com

References

- [1] Yan C, Cai R, Wang Y and Xu J. Successful stenting of bilateral main pulmonary artery

stenoses associated with Wegener's granulomatosis. *Eur Heart J Cardiovasc Imaging* 2025; 26: 372.

[2] Constantine A, Dimopoulos K, Gerges C and Lang IM. Peripheral pulmonary artery stenosis in adults: a novel type of pulmonary vascular disease with a strong genetic background. *Eur Respir J* 2023; 62: 2302085.

[3] Huang Z, Dong F, Wang M, Hu F and Liu X. Comparison of long-term survival after endovascular treatment versus medical therapy in patients with Takayasu's arteritis and pulmonary artery stenosis. *Clin Exp Rheumatol* 2023; 41: 887-892.

[4] Yanagisawa R, Kataoka M, Inami T, Fukuda K, Yoshino H and Satoh T. Intravascular imaging-guided percutaneous transluminal pulmonary angioplasty for peripheral pulmonary stenosis and pulmonary Takayasu arteritis. *J Heart Lung Transplant* 2016; 35: 537-540.

[5] Nagata H, Kanou T, Fukui E, Kimura T, Ose N, Funaki S, Minami M, Taira M, Ueno T, Miyagawa S and Shintani Y. A case of surgical pulmonary artery plasty for pulmonary artery stenosis after right single-lung transplantation. *Gen Thorac Cardiovasc Surg Cases* 2023; 2: 30.

[6] Milzi A, Landi A, Dettori R, Burgmaier K, Reith S and Burgmaier M. Multimodal intravascular imaging of the vulnerable coronary plaque. *Echocardiography* 2024; 41: e70035.

[7] Ren Y, Chu X, Senarathna J, Bhargava A, Grayson WL and Pathak AP. Multimodality imaging reveals angiogenic evolution in vivo during calvarial bone defect healing. *Angiogenesis* 2024; 27: 105-119.

[8] Parikh MJ and Madder RD. Near-infrared spectroscopy-guided percutaneous coronary intervention: practical applications and available evidence. *Interv Cardiol Clin* 2023; 12: 257-268.

[9] Ihdayhid AR, Tzimas G, Peterson K, Ng N, Mirza S, Maehara A and Safian RD. Diagnostic performance of AI-enabled plaque quantification from coronary CT angiography compared with intravascular ultrasound. *Radiol Cardiothorac Imaging* 2024; 6: e230312.

[10] Galiè N, Hoeper MM, Humbert M, Torbicki A, Vachiery JL, Barbera JA, Beghetti M, Corris P, Gaine S, Gibbs JS, Gomez-Sanchez MA, Jondeau G, Klepetko W, Opitz C, Peacock A, Rubin L, Zellweger M and Simonneau G. Guidelines for the diagnosis and treatment of pulmonary hypertension: the task force for the diagnosis and treatment of pulmonary hypertension of the European Society of Cardiology (ESC) and the European Respiratory Society (ERS), endorsed by the International Society of Heart and Lung Transplantation (ISHLT). *Eur Heart J* 2009; 30: 2493-2537.

[11] Tonelli AR, Ahmed M, Hamed F and Prieto LR. Peripheral pulmonary artery stenosis as a cause of pulmonary hypertension in adults. *Pulm Circ* 2015; 5: 204-210.

[12] Cao Y, Singh V, Jiang N, Wei R, Jiang K and Wang H. Stenting for pulmonary artery stenosis resistant to balloon pulmonary angioplasty in chronic thrombo-embolic pulmonary hypertension: a bail out strategy. *Eur Heart J Case Rep* 2021; 5: ytab071.

[13] Higuchi S, Ota H, Yaoita N, Kamada H, Takagi H, Satoh T, Yasuda S and Takase K. Update on the roles of imaging in the management of chronic thromboembolic pulmonary hypertension. *J Cardiol* 2023; 81: 297-306.

[14] Vonk Noordegraaf A, Westerhof BE and Westerhof N. The relationship between the right ventricle and its load in pulmonary hypertension. *J Am Coll Cardiol* 2017; 69: 236-243.

[15] Roller FC, Schüssler A, Hasse A, Kriechbaum S, Richter M, Guth S, Tello K, Breithecker A, Liebetrau C, Hamm CW, Mayer E, Seeger W, Krombach GA and Wiedenroth CB. Effects of BPA on right ventricular mechanical dysfunction in patients with inoperable CTEPH - A cardiac magnetic resonance study. *Eur J Radiol* 2022; 147: 110111.

[16] Alagha Z, Bills E, Alastal M, Ghallab M, Al-Astal A and Mahdi A. The harms of unnecessary CT pulmonary angiography: a case report and literature review. *J Investig Med High Impact Case Rep* 2024; 12: 23247096241258603.

[17] Kumar G, Effoe VS, Kumar A, Verma I and Sachdeva R. Intravascular ultrasound-guided catheter-based aspiration thrombectomy in patients with acute submassive pulmonary embolism: a case series. *Cardiovasc Revasc Med* 2022; 36: 138-143.

[18] Li X, Ge Z, Kan J, Anjum M, Xie P, Chen X, Khan HS, Guo X, Saghir T, Chen J, Gill BUA, Guo N, Sheiban I, Raza A, Wei Y, Chen F, Mintz GS, Zhang JJ, Stone GW and Chen SL. Intravascular ultrasound-guided versus angiography-guided percutaneous coronary intervention in acute coronary syndromes (IVUS-ACS): a two-stage, multicentre, randomised trial. *Lancet* 2024; 403: 1855-1865.

[19] Ichimura K, Boehm M, Andruska AM, Zhang F, Schimmel K, Bonham S, Kabiri A, Kheyfets VO, Ichimura S, Reddy S, Mao Y, Zhang T, Wang GX, Santana EJ, Tian X, Esaafri I, Vinh R, Tian W, Nicolls MR, Yajima S, Shudo Y, MacArthur JW, Woo YJ, Metzger RJ and Spiekerkoetter E. 3D imaging reveals complex microvascular remodeling in the right ventricle in pulmonary hypertension. *Circ Res* 2024; 135: 60-75.

[20] Smits AJ, Isebia K, Combee-Duffy C, van der Wal S, Nossent EJ, Boonstra A, Vonk-Noordegraaf A, Bogaard HJ and Serné EH. Low nailfold

capillary density in patients with pulmonary arterial hypertension and chronic thromboembolic pulmonary hypertension: biomarker of clinical outcome? *Sci Rep* 2024; 14: 19467.

[21] Arvanitaki A, Giannakoulas G, Triantafyllidou E, Feloukidis C, Boutou AK, Garyfallos A, Karvounis H and Dimitroulas T. Peripheral microangiopathy in precapillary pulmonary hypertension: a nailfold video capillaroscopy prospective study. *Respir Res* 2021; 22: 27.

[22] de Gregorio C, Trimarchi G, Faro DC, Poleggi C, Teresi L, De Gaetano F, Zito C, Lofrumento F, Koniari I, Licordari R, Kounis NG, Monte IP and Di Bella G. Systemic vascular resistance and myocardial work analysis in hypertrophic cardiomyopathy and transthyretin cardiac amyloidosis with preserved left ventricular ejection fraction. *J Clin Med* 2024; 13: 1671.

[23] Elbaz MSM, Shafeqhat M, Freed BH, Sarnari R, Zilber Z, Avery R, Markl M, Allen BD and Carr J. 3D vortex-energetics in the left pulmonary artery for differentiating pulmonary arterial hypertension and pulmonary venous hypertension groups using 4D flow MRI. *J Magn Reson Imaging* 2025; 61: 2130-2143.

[24] Yamaguchi N, Hirata Y, Nishio S, Takahashi T, Saijo Y, Kadota M, Ise T, Yamaguchi K, Yagi S, Yamada H, Soeki T, Wakatsuki T, Sata M and Kusunose K. Pulmonary pressure-flow responses to exercise in heart failure treated with angiotensin receptor neprilysin inhibitor. *Int J Cardiol* 2024; 400: 131789.

[25] Wang J, Dong Y, Zhao B and Liu K. Preoperative NT-proBNP and LVEF for the prediction of acute kidney injury after noncardiac surgery: a single-centre retrospective study. *BMC Anesthesiol* 2022; 22: 196.

[26] Gao X, Liu R, Wang P, Wang W and Zhao HQ. Relationship between NT-proBNP levels and left ventricular ejection fraction in patients with unstable angina and diabetes mellitus and preserved LVEF. *Int Heart J* 2022; 63: 821-827.

[27] Kimura T, Koeda Y, Ishida M, Numahata W, Yamaya S, Kikuchi S, Ishisone T, Goto I, Itoh T and Morino Y. Safety and feasibility of intravascular ultrasound-guided robotic percutaneous coronary intervention. *Coron Artery Dis* 2023; 34: 463-469.

[28] Gao X, Kan J, Wu Z, Anjun M, Chen X, Chen J, Sheiban I, Mintz GS, Zhang JJ, Stone GW and Chen SL. IVUS-guided vs angiography-guided PCI in patients with diabetes with acute coronary syndromes: the IVUS-ACS trial. *JACC Cardiovasc Interv* 2025; 18: 283-293.

[29] De Maria GL, Testa L, de la Torre Hernandez JM, Terentes-Printzios D, Emfietzoglou M, Scarsini R, Bedogni F, Spitzer E and Banning A. A multi-center, international, randomized, 2-year, parallel-group study to assess the superiority of IVUS-guided PCI versus qualitative angioguided PCI in unprotected left main coronary artery (ULMCA) disease: study protocol for OPTIMAL trial. *PLoS One* 2022; 17: e0260770.

[30] Aguirre AD, Arbab-Zadeh A, Soeda T, Fuster V and Jang IK. Optical coherence tomography of plaque vulnerability and rupture: JACC focus seminar part 1/3. *J Am Coll Cardiol* 2021; 78: 1257-1265.